

Inclusive hadronic distributions in jets and sub-jets with jet axis from color current

Redamy Pérez-Ramos^a

^aII. Institut für Theoretische Physik, Universität Hamburg,
Luruper Chaussee 149 22761 Hamburg, Germany

The hadronic k_{\perp} -spectrum and the gluon to quark average multiplicity ratio $r = N_g/N_q$ inside a high energy sub-jet are determined from a precise definition of the jet axis, including corrections of relative magnitude $\mathcal{O}(\sqrt{\alpha_s})$ with respect to the Modified Leading Logarithmic Approximation (MLLA), in the limiting spectrum approximation (assuming an infrared cut-off $Q_0 = \Lambda_{\text{QCD}}$). The results for the k_{\perp} -spectrum in the limiting spectrum approximation are found to be, after normalization, in impressive agreement with measurements by the CDF collaboration and the ratio has not been measured yet.

1. Introduction

The collimation of hadrons in jets is a basic phenomenon of high energy collisions and its quantitative understanding is an important task for QCD. Simple differential characteristics of a jet are their energy and multiplicity angular profiles. The collimation of energy and multiplicity in the jet follows from the dominance of gluon bremsstrahlung processes in the parton cascade evolution. Whereas the former is more sensitive to the hard processes inside a jet the second one is sensitive to the soft parton emissions from the primary parton.

The characteristics of soft particle production, such as particle multiplicities, inclusive distributions and correlation functions, are derived in QCD in the Double Logarithmic Approximation (DLA) and the Modified Leading Logarithmic Approximation (MLLA) (for review, see [1]), which takes into account the leading double logarithmic terms and the single logarithmic corrections. These azimuthally averaged quantities can be obtained from an evolution equation for the generating functional of the parton cascade. This equation provides also Next-to-MLLA (NMLLA) corrections taking into account energy conservation of parton splittings with increased accuracy. The corresponding hadronic observables can be obtained using the concept of Local Parton

Hadron Duality (LPHD) [2], which has turned out a successful description of many hadronic phenomena (see, e.g. [3]).

The inclusive k_{\perp} -distribution of particles inside a sub-jet with respect to the jet axis has been computed at MLLA accuracy in the limiting spectrum approximation [4], *i.e.* assuming an infrared cutoff Q_0 equal to Λ_{QCD} ($\lambda \equiv \ln(Q_0/\Lambda_{\text{QCD}}) = 0$) (for a review, see also [1]). MLLA corrections, of relative magnitude $\mathcal{O}(\sqrt{\alpha_s})$, were shown to be quite substantial [4]. Therefore, corrections of order $\mathcal{O}(\alpha_s)$, that is NMLLA, have been incorporated in [5,6].

Another characteristic prediction of QCD is the asymptotic increase of the mean average particle multiplicity in a gluon jet over the quark jet by the ratio of color factors $r = N_g/N_q \rightarrow N_c/C_F = 9/4$, which is also modified by the similar set of corrections $\mathcal{O}(\sqrt{\alpha_s})$ [7,8,9]. In particular, this analysis has been extended to multiparticle production inside sub-jets with a precise prescription of the jet axis, which has been, for both observables, identified with the direction of the energy flux [10].

The starting point of this analysis is the MLLA Master Equation for the *Generating Functional* (GF) $Z = Z(u)$ of QCD jets [1], where $u = u(k)$ is a certain probing function and k , the four-momentum of the outgoing parton. Together

with the initial condition at threshold, the GF determines the jet properties at all energies. Within this logic, the leading (DLA, $\mathcal{O}(\sqrt{\alpha_s})$) and next-to-leading (MLLA, $\mathcal{O}(\alpha_s)$) approximations are complete. The next terms (NMLLA, $\mathcal{O}(\alpha_s^{3/2})$) are not complete but they include an important contribution which takes into account energy conservation and an improved behavior near threshold. Indeed, some results for such NMLLA terms have been studied previously for global observables and have been found to better account for recoil effects and to drastically affect multi-particle production [11,12].

The main results of this work have been published in [5,6,10]. Experimentally, the CDF collaboration at the Tevatron reported on k_\perp -distributions of unidentified charged hadrons in jets produced in $p\bar{p}$ collisions at $\sqrt{s} = 1.96$ TeV [13].

2. MLLA evolution equations

2.1. Inclusive spectrum

We start by writing the MLLA evolution equations for the fragmentation function $D_B^h(x/z, zE\Theta_0, Q_0)$ of a parton B (energy zE and transverse momentum $k_\perp = zE\Theta_0$) into a gluon (represented by a hadron h (energy xE) according to LPHD [2]) inside a jet A of energy E for the process depicted in Fig. 1. As a conse-

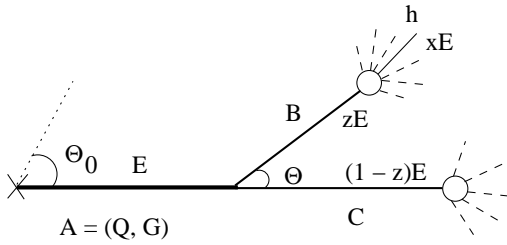


Figure 1. Parton A with energy E splits into parton B (respectively C) with energy zE (respectively, $(1-z)E$) which fragments into a hadron h with energy xE .

quence of angular ordering in parton cascading, partonic distributions inside a quark and gluon jet, $Q, G(z) = x/z D_{Q,G}^h(x/z, zE\Theta_0, Q_0)$, obey the system of two coupled equations [14] (the subscript y denotes $\partial/\partial y$) following from the MLLA master equation [1]

$$\begin{aligned} Q_y &= \int_0^1 dz \frac{\alpha_s}{\pi} \Phi_q^g(z) \left[(Q(1-z) - Q) + G(z) \right] \\ G_y &= \int_0^1 dz \frac{\alpha_s}{\pi} \left[\Phi_g^g(z) (G(z) + G(1-z) \right. \\ &\quad \left. - G) + n_f \Phi_g^q(z) (2Q(z) - G) \right]. \end{aligned} \quad (2)$$

$\Phi_A^B(z)$ denotes the Dokshitzer-Gribov-Lipatov-Altarelli-Parisi (DGLAP) splitting functions [1],

$$\begin{aligned} \Phi_q^g(z) &= C_F \left(\frac{2}{z} + \phi_q^g(z) \right), \\ \Phi_g^g(z) &= T_R [z^2 + (1-z)^2], \\ \Phi_g^q(z) &= 2N_c \left(\frac{1}{z} + \phi_g^q(z) \right), \end{aligned} \quad (3)$$

where $\phi_q^g(z) = z-2$ and $\phi_g^q(z) = (z-1)(2-z(1-z))$ are regular as $z \rightarrow 0$, $C_F = (N_c^2 - 1)/2N_c$, $T_R = n_f/2$ ($N_c = 3$ is the number of colors for $SU(3)_c$ and $n_f = 3$ is the number of light flavors we consider). The running coupling of QCD (α_s) is given by

$$\alpha_s = \frac{2\pi}{4N_c\beta_0(\ell + y + \lambda)}, \quad 4N_c\beta_0 = \frac{11}{3}N_c - \frac{4}{3}T_R$$

and

$$\ell = (1/x), \quad y = \ln(k_\perp/Q_0), \quad \lambda = \ln(Q_0/\Lambda_{\text{QCD}}),$$

where Q_0 is the collinear cut-off parameter. Moreover,

$$\begin{aligned} G &\equiv G(1) = x D_G^h(x, E\Theta_0, Q_0), \\ Q &\equiv Q(1) = x D_Q^h(x, E\Theta_0, Q_0). \end{aligned} \quad (4)$$

At small $x \ll z$, the fragmentation functions behave as

$$B(z) \approx \rho_B^h \left(\ln \frac{z}{x}, \ln \frac{zE\Theta_0}{Q_0} \right) = \rho_B^h(\ln z + \ell, y),$$

ρ_B^h being a slowly varying function of two logarithmic variables $\ln(z/x)$ and y that describes

the ‘‘hump-backed’’ plateau [15]. Since recoil effects should be largest in hard parton splittings, the strategy followed in this work is to perform Taylor expansions (first advocated for in [16]) of the non-singular parts of the integrands in (1,2) in powers of $\ln z$ and $\ln(1-z)$, both considered small with respect to ℓ in the hard splitting region $z \sim 1-z = \mathcal{O}(1)$

$$B(z) = B(1) + B_\ell(1) \ln z + \mathcal{O}(\ln^2 z) \quad (5)$$

with $z \leftrightarrow 1-z$. Each ℓ -derivative giving an extra $\sqrt{\alpha_s}$ factor (see [14]), the terms $B_\ell(1) \ln z$ and $B_\ell(1) \ln(1-z)$ yield NMLLA corrections to the solutions of (2). Making use of (5), after integrating over the regular parts of the DGLAP splitting functions, while keeping the singular terms unchanged, one gets after some algebra ($\gamma_0^2 = 2N_c\alpha_s/\pi$) [5,6]

$$Q(\ell, y) = \delta(\ell) + \frac{C_F}{N_c} \int_0^\ell d\ell' \int_0^y dy' \gamma_0^2(\ell' + y') \times (6)$$

$$\left[1 - \tilde{a}_1 \delta(\ell' - \ell) + \tilde{a}_2 \delta(\ell' - \ell) \psi_\ell(\ell', y') \right] G(\ell', y'),$$

$$G(\ell, y) = \delta(\ell) + \int_0^\ell d\ell' \int_0^y dy' \gamma_0^2(\ell' + y') \times$$

$$\left[1 - a_1 \delta(\ell' - \ell) a_2 \delta(\ell' - \ell) \psi_\ell(\ell', y') \right] G(\ell', y'), \quad (7)$$

where the constants take the values $a_1 \approx 0.935$, $\tilde{a}_1 = 3/4$, $a_2 \approx 0.08$ and $\tilde{a}_2 \approx 0.42$ for $n_f = 3$. Defining $F(\ell, y) = \gamma_0^2(\ell + y)G(\ell, y)$, we can exactly solve the self-contained equation (7) by performing the inverse Mellin transform:

$$F(\ell, y) = \int \frac{d\omega d\nu}{(2\pi i)^2} e^{\omega\ell} e^{\nu y} \mathcal{F}(\omega, \nu), \quad (8)$$

such that the NMLLA solution reads

$$G(\ell, y) = (\ell + y + \lambda) \int \frac{d\omega d\nu}{(2\pi i)^2} e^{\omega\ell} e^{\nu y} \int_0^\infty \frac{ds}{\nu + s}$$

$$\times \left(\frac{\omega(\nu + s)}{(\omega + s)\nu} \right)^{\sigma_0} \left(\frac{\nu}{\nu + s} \right)^{\sigma_1 + \sigma_2} e^{-\sigma_3 s}, \quad (9)$$

where

$$\sigma_0 = \frac{1}{\beta_0(\omega - \nu)}, \quad \sigma_1 = \frac{a_1}{\beta_0},$$

and

$$\sigma_2 = -\frac{a_2}{\beta_0}(\omega - \nu), \quad \sigma_3 = -\frac{a_2}{\beta_0} + \lambda.$$

As can be seen, the NMLLA coefficient a_2 is very small. Therefore, the NMLLA solution (9) of (7) can be approximated by the MLLA solution of $G(\ell, y)$ (*i.e.* taking $a_2 \approx 0$), which is used in the following to compute the inclusive k_\perp -distribution. As demonstrated in [14], taking the limits $a_2 \approx 0$ and $\lambda \approx 0$ in (9), the integral representation can be reduced to the known MLLA formula, which can be written in terms of Bessel series in the limiting spectrum approximation [1]. To get a quantitative idea on the difference between MLLA and NMLLA gluon inclusive spectrum, the reader is reported to the appendix B of [5]. The magnitude of \tilde{a}_2 , however, indicates that the NMLLA corrections to the inclusive quark jet spectrum may not be negligible and should be taken into account. After solving (7), the solution of (6) reads

$$Q(\ell, y) = \frac{C_F}{N_c} \left[G(\ell, y) + (a_1 - \tilde{a}_1) G_\ell(\ell, y) \right. \\ \left. + (a_1(a_1 - \tilde{a}_1) + \tilde{a}_2 - a_2) G_{\ell\ell}(\ell, y) \right] \quad (10)$$

It differs from the MLLA expression given in [4] by the term proportional to $G_{\ell\ell}$, which can be deduced from the subtraction of $(C_F/N_c) \times (7)$ to Eq. (6).

2.2. Particle mean average multiplicity

Integrating the system (1,2) over the energy fraction x leads the average multiplicity of particles produced in the jet:

$$N_A(Y_{\Theta_0}) = \int_0^1 dx D_A(x, E\Theta_0, Q_0).$$

where $Y_{\Theta_0} \equiv \ell + y = \ln(E\Theta_0/Q_0)$. Therefore, an equivalent system of two-coupled evolution equations can be deduced and expanded, following the same logic that led to (6,7). However, in this case, the expansion in $\sqrt{\alpha_s}$ is performed for $Y_\Theta \gg \ln z \sim \ln(1-z)$, where similarly, $z \sim 1$. We limit ourselves here to the NMLLA expression of r that reads

$$r = \frac{N_g}{N_q} = r_0(1 - r_1\gamma_0 - r_2\gamma_0^2) + \mathcal{O}(\gamma_0^3), \quad (11)$$

where the asymptotic value of r is $r_0 = N_c/C_F = 9/4$. The MLLA term r_1 has been calculated in

[7]. The coefficients r_k can be obtained from the Taylor expansions of $N_A^h(Y_\Theta + \ln x)$ and $N_A^h(Y_\Theta + \ln(1-x))$ for $Y_\Theta \gg \ln x$ and $Y_\Theta \gg \ln(1-x)$ in the evolution equations [16]. The values of r_k for $n_f = 3$ read $r_1 = 0.185$ and $r_2 = 0.426$ [16]. The NMLLA solution for the mean multiplicity in a gluon jet is found as [16]

$$N_g^h(Y_\Theta) \simeq \mathcal{K} (Y_\Theta)^{-c_1/\beta_0} \times \exp\left(\frac{2}{\sqrt{\beta_0}}\sqrt{Y_\Theta} - \frac{2c_2}{\beta_0^{3/2}\sqrt{Y_\Theta}}\right) \quad (12)$$

with $c_1 = 0.28$, $c_2 = 0.38$ for $n_f = 3$ and \mathcal{K} , the LPHD normalization factor. The pre-exponential term $(Y_\Theta)^{-c_1/\beta_0}$ is the MLLA contribution to N_g^h , while the one $\propto c_2$, the NMLLA one.

3. Single inclusive k_\perp -distribution of charged hadrons and the gluon to quark mean average multiplicity ratio r at NMLLA

3.1. Inclusive k_\perp -distribution

Computing the single inclusive k_\perp -distribution and the ratio $r = N_g/N_q$ inside a sub-jet requires the definition of the jet axis. The starting point of our approach consists in considering the correlation between two particles (h1) and (h2) of energies E_1 and E_2 which form a relative angle Θ inside one jet of total opening angle $\Theta_0 > \Theta$ [17]. Weighting over the energy E_2 of particle (h2), this relation leads to the correlation between the particle (h=h1) and the energy flux, which we identify with the jet axis (see Fig. 2) [4]. Thus, the correlation and the relative transverse momentum k_\perp between (h1) and (h2) are replaced by the correlation, and transverse momentum of (h1) with respect to the direction of the energy flux. Finally, we obtain the double differential spectrum $d^2N/dx d\Theta$ of a hadron produced with energy $E_1 = xE$ at angle Θ (or $k_\perp \approx xE\Theta$) with respect to the jet axis. As demonstrated in [4], the correlation reads

$$\frac{d^2N}{dx d\ln\Theta} = \frac{d}{d\ln\Theta} F_{A_0}^h(x, \Theta, E, \Theta_0), \quad (13)$$

where $F_{A_0}^h$ is given by the convolution of two fragmentation functions

$$F_{A_0}^h \equiv \sum_{A=g,q} \int_x^1 du D_{A_0}^A(u, E\Theta_0, uE\Theta) \times D_A^h\left(\frac{x}{u}, uE\Theta, Q_0\right), \quad (14)$$

u being the energy fraction of the intermediate parton A . $D_{A_0}^A$ describes the probability to emit A with energy uE off the parton A_0 (which initiates the jet), taking into account the evolution of the jet between Θ_0 and Θ . D_A^h describes the probability to produce the hadron h off A with energy fraction x/u and transverse momentum $k_\perp \approx uE\Theta \geq Q_0$ (see Fig. 2). As discussed in

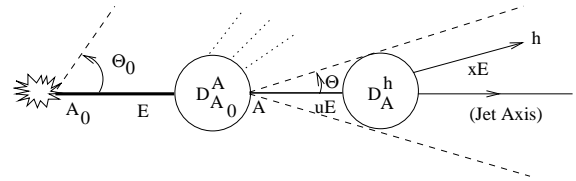


Figure 2. Inclusive production of hadron h at angle Θ inside a high energy jet of total opening angle Θ_0 and energy E .

[4], the convolution (14) is dominated by $u \sim 1$ and therefore $D_{A_0}^A(u, E\Theta_0, uE\Theta)$ is determined by the DGLAP evolution [1]. On the contrary, the distribution $D_A^h\left(\frac{x}{u}, uE\Theta, Q_0\right)$ at low $x \ll u$ reduces to the hump-backed plateau,

$$\tilde{D}_A^h(\ell + \ln u, y) \stackrel{x \ll u}{\approx} \rho_A^h(\ell + \ln u, Y_\Theta + \ln u), \quad (15)$$

with $Y_\Theta = \ell + y = \ln(E\Theta/Q_0)$. Performing the Taylor expansion of \tilde{D} to the second order in $(\ln u)$ and plugging it into Eq. (14) leads to

$$F_{g,q}^h(\ell, y) = \frac{1}{N_c} \langle C \rangle_{g,q}(\ell, y) G(\ell, y). \quad (16)$$

where $\langle C \rangle_{g,q}$ can be written in the symbolic way

$$\langle C \rangle_{g,q}(\ell, y) \simeq f_0(\ell, y) + f_1(\ell, y) \sqrt{\alpha_s} + f_2(\ell, y) \alpha_s, \quad (17)$$

where f_k follow from the DGLAP evolution equations [1] and can be symbolically written as

$$f_k \simeq \int_x^1 du u (\ln u)^k D_{A_0}^A(u, E\Theta_0, uE\Theta) \quad (18)$$

and corrections $\mathcal{O}(\alpha_s^{n/2})$ from the n -logarithmic derivatives of the inclusive spectrum:

$$\frac{1}{D_A} \frac{\partial^n D_A}{\partial \ell^n} \simeq \mathcal{O}(\alpha_s^{n/2}).$$

The exact formulæ of the color currents are reported in [4,5,6]. Indeed, since soft particles are less sensible to the energy balance, the correlation (14) disappears for these particles, leading to the sequence of factorized terms written in (17). The first two terms in Eq. (17) correspond to the MLLA distribution calculated in [4] when \tilde{D}_A^h is evaluated at NLO and its derivative at LO. NM-LLA corrections arise from their respective calculation at NNLO and NLO, and, mainly in practice, from the third term, which was exactly computed in [5,6]. Indeed, since x/u is small, the inclusive spectrum $\tilde{D}_A^h(\ell, y)$ with $A = G, Q$ are given by the solutions (9) and (10) of the next-to-MLLA evolution equations (6) and (7) respectively. However, because of the smallness of the coefficient a_2 , $G(\ell, y)$ shows no significant difference from MLLA to NMLLA. As a consequence, we use the MLLA expression (9) for $G(\ell, y)$ with $a_2 = 0$, and the NMLLA (10) for $Q(\ell, y)$. The functions F_g^h and F_q^h are related to the gluon distribution *via* the color currents $\langle C \rangle_{g,q}$ which can be seen as the average color charge carried by the parton A due to the DGLAP evolution from A_0 to A .

This calculation has also been extended beyond the limiting spectrum, $\lambda \neq 0$, to take into account hadronization effects in the production of “massive” hadrons, $m = \mathcal{O}(Q_0)$ [18]. We used, accordingly, the more general MLLA solution of (7) with $a_2 = 0$ for an arbitrary $\lambda \neq 0$, which can only be performed numerically. The NMLLA (normalized) corrections to the MLLA result are displayed in Fig. 3 for different values $\lambda = 0, 0.5, 1$. It clearly indicates that the larger λ , the smaller the NMLLA corrections. In particular, they can be as large as 30% at the limiting spectrum ($\lambda = 0$) but no more than 10%

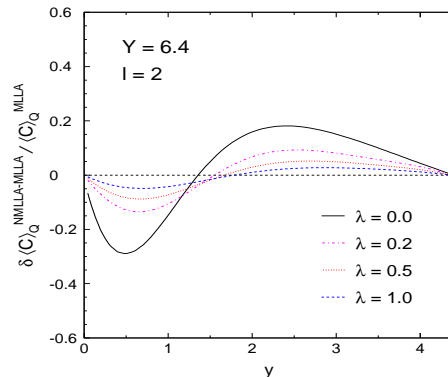


Figure 3. NMLLA corrections to the color current of a quark jet with $Y_{\Theta_0} = 6.4$ and $\ell = 2$ for various values of λ .

for $\lambda = 0.5$. This is not surprising since $\lambda \neq 0$ ($Q_0 \neq \Lambda_{\text{QCD}}$) reduces the parton emission in the infrared sector and, thus, higher-order corrections.

The double differential spectrum ($d^2N/d\ell dy$) can now be determined from the NMLLA color currents (17) by using the quark and gluon distributions. Integrating over ℓ leads to the single inclusive y -distribution (or k_{\perp} -distribution) of hadrons inside a quark or a gluon jet:

$$\left(\frac{dN}{dy} \right)_{A_0} = \int_{\ell_{\min}}^{Y_{\Theta_0}-y} d\ell \left(\frac{d^2N}{d\ell dy} \right)_{A_0}. \quad (19)$$

The MLLA framework does not specify down to which values of ℓ (up to which values of x) the double differential spectrum ($d^2N/d\ell dy$) should be integrated over. Since ($d^2N/d\ell dy$) becomes negative (non-physical) at small values of ℓ (see e.g. [4]), we chose the lower bound ℓ_{\min} so as to guarantee the positiveness of ($d^2N/d\ell dy$) over the whole $\ell_{\min} \leq \ell \leq Y_{\Theta_0}$ range (in practice, $\ell_{\min}^g \sim 1$ and $\ell_{\min}^q \sim 2$). Having successfully computed the single k_{\perp} -spectra including NMLLA corrections, we now compare the result with existing data. The CDF collaboration at the Tevatron recently reported on preliminary measurements over a wide range of jet hardness, $Q = E\Theta_0$,

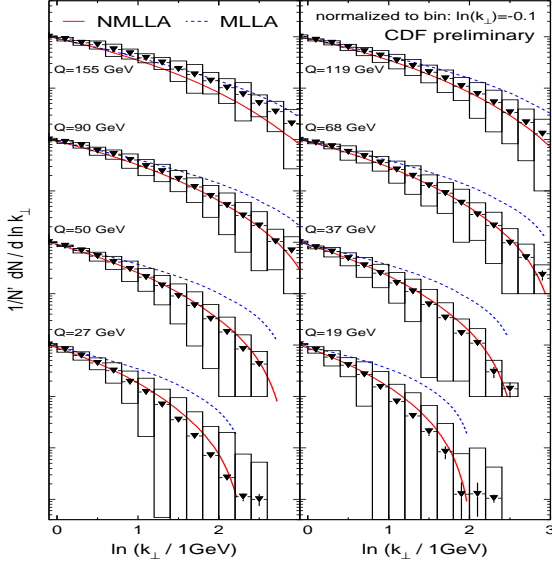


Figure 4. CDF preliminary results for the inclusive k_{\perp} distribution at various hardness Q in comparison to MLLA and NMLLA predictions at the limiting spectrum ($Q_0 = \Lambda_{QCD}$); the boxes are the systematic errors.

in $p\bar{p}$ collisions at $\sqrt{s} = 1.96$ TeV [13]. CDF data, including systematic errors, are plotted in Fig. 4 together with the MLLA predictions of [4] and the present NMLLA calculations, both at the limiting spectrum ($\lambda = 0$) and taking $\Lambda_{QCD} = 250$ MeV. The experimental distributions suffering from large normalization errors, data and theory are normalized to the same bin, $\ln(k_{\perp}/1 \text{ GeV}) = -0.1$. The agreement between the CDF results and the NMLLA distributions over the whole k_{\perp} -range is particularly good. In contrast, the MLLA predictions prove reliable in a much smaller k_{\perp} interval. At fixed jet hardness (and thus Y_{Θ_0}), NMLLA calculations prove accordingly trustable in a much larger x interval.

Finally, the kt -distribution is determined with respect to the jet energy flow (which includes a summation over secondary hadrons in energy-energy correlations). In experiments, instead, the

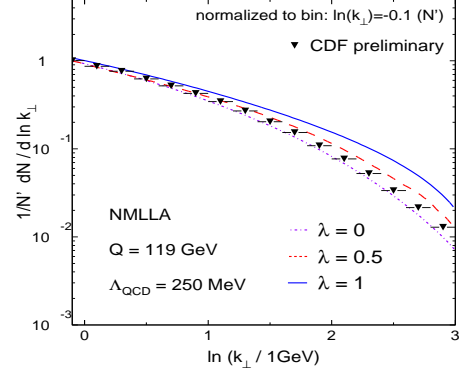


Figure 5. CDF preliminary results ($Q = 119$ GeV) for inclusive k_{\perp} distribution compared with NMLLA predictions beyond the limiting spectrum.

jet axis is determined exclusively from all particles inside the jet. The question of the matching of these two definitions goes beyond the scope of this letter. The NMLLA k_{\perp} -spectrum has also been calculated beyond the limiting spectrum, by plugging (9) with $a_2 = 0$ into (19), as illustrated in Fig. 5. However, the best description of CDF preliminary data is reached at the limiting spectrum, or at least for small values of $\lambda < 0.5$, which is not too surprising since these inclusive measurements mostly involve pions. Identifying produced hadrons would offer the interesting possibility to check a dependence of the shape of k_{\perp} -distributions on the hadron species, such as the one predicted in Fig. 5. Moreover, the softening of the k_{\perp} -spectra with increasing hadron masses predicted in Fig. 5 is an observable worth to be measured, as this would provide an additional and independent check of the LPHD hypothesis beyond the limiting spectrum. This could only be achieved if the various species of hadrons inside a jet can be identified experimentally. Fortunately, it is likely to be the case at the LHC, where the ALICE [19] and CMS [20] experiments at the Large Hadron Collider have good identification capabilities at not too large transverse

momenta.

3.2. Ratio $r = N_g/N_q$

Integrating (14) over the energy fraction x yields the corresponding sub-jet multiplicity $\hat{N}_{A_0}^h$ of hadrons inside the angular range $\Theta < \Theta_0$ of the jet A_0 [10]

$$\hat{N}_{A_0}^h(\Theta; E, \Theta_0) \approx \sum_{A=q,g} \int_{u_0}^1 du u D_{A_0}^A(u, E\Theta_0, uE\Theta) \times N_A^h(uE\Theta, Q_0), \quad (20)$$

where N_A^h is the number of hadrons (partons at scale Q_0) produced inside the sub-jet A of total virtuality $uE\Theta \geq Q_0$ and $u_0 = Q_0/E\Theta$. Within the leading parton approximation, we expand the multiplicity $N_A^h(uE\Theta, Q_0)$ in (20) at $u \sim 1$. Similarly to the logic applied in (15) for the computation of the k_\perp -distribution, we take the logarithmic dependence of the average multiplicity N_A^h , such that for $\ln u \ll Y_\Theta \equiv \ln(E\Theta/Q_0)$ and $E\Theta \gg \Lambda$, one obtains the average multiplicity $\hat{N}_{A_0}^h(Y_{\Theta_0}, Y_\Theta)$ of soft hadrons within the sub-jet of opening angle Θ with respect to the energy flow

$$\hat{N}_{q,g}^h(Y_{\Theta_0}, Y_\Theta) \approx \frac{1}{N_c} \langle C \rangle_{q,g}(Y_{\Theta_0}, Y_\Theta) N_g^h(Y_\Theta), \quad (21)$$

where $N_g^h(Y_\Theta)$ is written in (12) and $\langle C \rangle_{q,g}(Y_{\Theta_0}, Y_\Theta)$ is the average color current of partons forming the energy flux. We write the color current as

$$\langle C \rangle_{q,g}(Y_{\Theta_0}, Y_\Theta) \simeq \tilde{f}_0 + \tilde{f}_1 \sqrt{\alpha_s} + \tilde{f}_2 \alpha_s,$$

where $\tilde{f}_k \equiv \tilde{f}_k(Y_{\Theta_0}, Y_\Theta)$ follow from (11) and (18) and corrections $\mathcal{O}(\alpha_s^{n/2})$ from the logarithmic derivatives of the average multiplicity (12):

$$\frac{1}{N_A} \frac{d^n N_A}{dY_\Theta^n} \simeq \alpha_s^{n/2}.$$

The exact formulæ of $\langle C \rangle_{q,g}(Y_{\Theta_0}, Y_\Theta)$ are given in the appendix of [10]. The ratio of the gluon to the quark jet average multiplicity reads

$$\frac{\hat{N}_g^h}{\hat{N}_q^h}(Y_{\Theta_0}, Y_\Theta) = \frac{\langle C \rangle_g(Y_{\Theta_0}, Y_\Theta)}{\langle C \rangle_q(Y_{\Theta_0}, Y_\Theta)}.$$

For this quantity, in the limit $\Theta \rightarrow \Theta_0$, the appropriate ratio (11) $r = \frac{N_g}{N_q} = r_0(1 - r_1\gamma_0 - r_2\gamma_0^2)$ is recovered.

Next we study the consequences for the behavior of the ratio at full angles $\Theta_0 \sim 1$ and for sub-jets at reduced angles Θ . Results for the ratio using our formulae for the color currents $\langle C \rangle_{q,g}$ [10] are depicted in Fig. 6. The full line shows the ratio (11) for an isolated A_0 jet as a function of $Y_{\Theta_0} = \ln(E\Theta_0/Q_0)$. The three curves below cor-

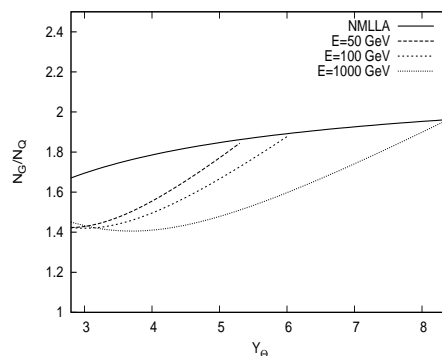


Figure 6. Multiplicity ratio N_g/N_q for jets and sub-jets as function of energy variable $Y = \ln(E\Theta/Q_0)$.

respond to the sub-jet energies $E = 50, 100, 1000$ GeV and the intersection points with (11) to the limit $\Theta \rightarrow \Theta_0$. Therefore, the mixing of quark and gluon jets reduces the multiplicity in the gluon jet and increases it in the quark jet at sufficiently high energies and the effect from intermediate processes in the new definition of multiplicity ratio amounts to about 20% at a reduced energy scale $Y_\Theta \sim Y_{\Theta_0} - 2$.

4. Conclusion

We have studied a definition of the jet which arises from the 2-particle correlation. The jet axis corresponds to the energy weighted direction of particles in a given cone Θ_0 . In this way smaller angles (or transverse momenta) can be meaningfully determined.

The new effect from 2-particle correlations is the appearance of the “color current” in the result, which reflects the possibility of intermediate quark-gluon processes. We then studied the consequences of this analysis on the measurement of differential (k_{\perp} -distribution) and global (particle multiplicity) observables, where we have added MLLA and NMLLA corrections to the known LO results [1].

The single inclusive k_{\perp} -spectra is determined within this logic and the agreement between NMLLA predictions and CDF data in $p\bar{p}$ collisions at the Tevatron [13] is impressive, indicating very small overall non-perturbative corrections and giving further support to LPHD [2].

The main for the ratio $r = N_g/N_q$ reflects the possibility of intermediate quark-gluon processes. This effect can be seen by the scale breaking between jets and sub-jets at the same scale $E\Theta$ but different energies E and opening angles Θ . Typical effects are of the order of 20%. However, these effects on this observable have not been measured yet.

REFERENCES

1. Yu.L. Dokshitzer, V.A. Khoze, A.H. Mueller, S.I. Troyan, *Basics of Perturbative QCD*, (Editions Frontières, Gif-sur-Yvette, 1991).
2. Ya.I. Azimov, Yu.L. Dokshitzer, V.A. Khoze, S.I. Troian, *Similarity of Parton and Hadron Spectra in QCD Jets*, *Z. Phys C* **27** (1985) 65;
Yu.L. Dokshitzer, V.A. Khoze, S.I. Troian, *On the concept of local parton hadron duality*, *J. Phys. G* **17** (1991) 1585.
3. V.A. Khoze, W. Ochs, *Perturbative QCD approach to multi-particle production*, *Int. J. Mod. Phys. A* **12** (1997) 2949.
4. R. Pérez Ramos, B. Machet, *MLLA inclusive hadronic distributions inside one jet at high energy colliders*, [[hep-ph/0512236](#)], *JHEP* **04** (2006) 043.
5. R. Perez-Ramos, F. Arleo & B. Machet, *Next-to-MLLA corrections to single inclusive k_{\perp} distributions and two-particle correlations in a jet*, [[arXiv:0712.2212 \[hep-ph\]](#)], *Phys. Rev. D* **78** (2008) 014019.
6. F. Arleo, R. Pérez-Ramos, B. Machet: “Hadronic single inclusive k_{\perp} distributions inside one jet beyond MLLA”, [arXiv:07072391 \[hep-ph\]](#), *Phys. Rev. Lett.* **100** (2008) 052002.
7. A.H. Mueller, *Nucl. Phys. B* **241** (1984) 141; Erratum *ibid.*, **B 241** (1984) 141.
8. E.D. Malaza & B.R. Webber, *Phys. Lett. B* **149** (1984) 501.
9. I.M. Dremin, V.A. Nechitailo, *Mod. Phys. Lett. A* **9** (1994) 1471; *JETP Lett.* **58** (1993) 945.
10. Wolfgang Ochs & Redamy Perez-Ramos, “*Particle Multiplicity in Jets and Sub-jets with Jet Axis from Color Current.*”, [arXiv:0807.1082 \[hep-ph\]](#), published in *Phys.Rev.D* **78:034010,2008**.
11. Yu.L. Dokshitzer, *Improved QCD treatment of the KNO phenomenon*, *Phys. Lett. B* **305** (1993) 295.
12. F. Cuypers, K. Tesima, *Recoil effect on multiplicity correlation*, *Z. Phys. C* **54** (1992) 87.
13. CDF collaboration, T. Aaltonen *et al.*, *Measurement of the kT Distribution of Particles in Jets Produced in $p\bar{p}$ Collisions at $s^{(1/2)} = 1.96\text{-TeV}$* , [arXiv:0811.2820\[hep-ex\]](#).
14. R. Pérez Ramos, *Two particle correlations inside one jet at Modified Leading Logarithmic Approximation of Quantum Chromodynamics; I: Exact solution of the evolution equations at small x* , [[hep-ph/0605083](#)], *JHEP* **06** (2006) 019 and references therein.
15. Yu.L. Dokshitzer, V.S. Fadin, V.A. Khoze, *Coherent effects in the perturbative QCD parton jets*, *Phys. Lett. B* **115** (1982) 242;
Ya.I. Azimov, Yu.L. Dokshitzer, V.A. Khoze, S.I. Troian, *Humpbacked QCD Plateau in Hadron Spectra*, *Z. Phys. C* **31** (1986) 213;
C.P. Fong, B.R. Webber, *Higher order QCD corrections to hadron energy distribution in jets*, *Phys. Lett. B* **229** (1989) 289.
16. I.M. Dremin, *Quantum chromodynamics and multiplicity distributions*, [[hep-ph/9406231](#)], *Phys. Usp.* **37** (1994) 715;
ibid., *Usp. Fiz. Nauk* **164** (1994) 785;
I.M. Dremin, J.W. Gary, *Hadron multiplicities*, *Phys. Rep.* **349** (2001) 301;

- I.M. Dremin, V.A. Nechitailo, *Average multiplicities in gluon and quark jets in higher order perturbative QCD*, [hep-ex/9406002], Mod. Phys. Lett. **A9** (1994) 1471.
17. Yu.L. Dokshitzer, D.I. Dyakonov & S.I. Troyan, *Hard processes in Quantum Chromodynamics*, Phys. Rep. **58** (1980) 270.
 18. Yu.L. Dokshitzer, V.A. Khoze, S.I. Troian, *Phenomenology of the particle spectra in QCD jets in a modified leading logarithmic approximation*, Z. Phys. **C 55** (1992) 107;
Yu.L. Dokshitzer, V.A. Khoze, S.I. Troian, *Inclusive particle spectra from QCD cascades*, Int. J. Mod. Phys. **A 7** (1992) 1875;
V.A. Khoze, W. Ochs, J. Wosieck, *Analytical QCD and multi-particle production*, [hep-ph/0009298], and references therein.
 19. ALICE collaboration, *ALICE physics performance report, volume II*, B. Alessandro *et al.*, J. Phys. **G32** (2006) 1295.
 20. CMS collaboration, *CMS physics technical design report: Addendum on high density QCD with heavy ions*, D. d'Enterria (Ed.) *et al.*, J. Phys. **G34** (2007) 2307.